Challenges of Dynamic High Resolution Photoacoustic Tomography

Felix Lucka

University College London, UK

joint work with: Marta Betcke, Simon Arridge, Ben Cox, Nam Huynh, Edward Zhang and Paul Beard

Centre for Medical Image Computing

Münster, February 2, 2015

source: Wikimedia Commons

Production of acoustic waves by the thermalization of absorbed photons:

- A photon is absorbed by "chromophores"
- The energy is thermalized.
- Heating and cooling translate into local pressure changes.
- Pressure changes propagates as an acoustic wave.

History:

- Discovery in 1880 by Alexander Graham Bell.
- Nothing happened for 100 years.
- Lasers provide the high peak power, spectral purity and directionality to make use of it.
- Biomedical imaging since mid-1990s

Photoacoustic Imaging: Basic Principle

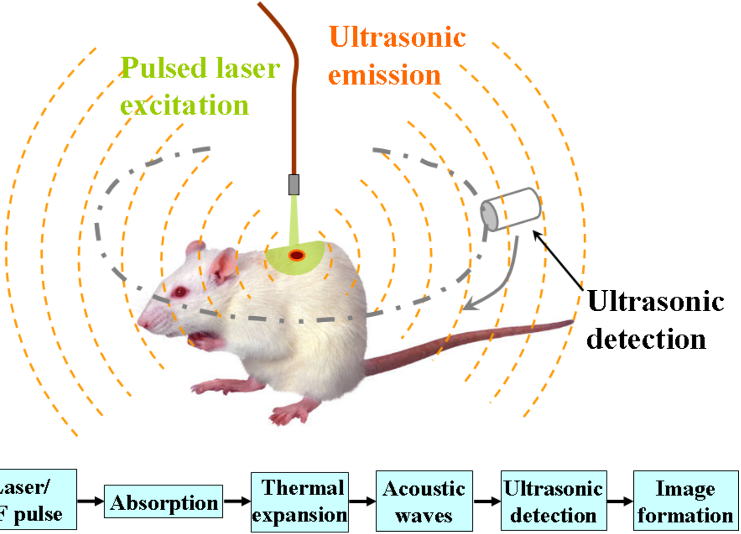

source: Wikimedia Commons

Photoacoustic Imaging: Contrast

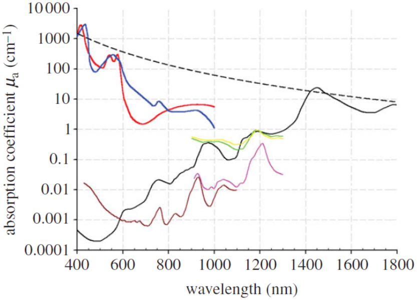

Figure 1. Absorption coefficient spectra of endogenous tissue chromophores. Oxyhaemoglobin (HbO_2), red line: (http://omlc.ogi.edu/spectra/hemoglobin/summary.html; 150 $\mathrm{g\,l^{-1}}$), deoxyhaemoglobin (HHb), blue line: (http://omlc.ogi.edu/spectra/hemoglobin/summary.html; 150 $\mathrm{g\,l^{-1}}$), water, black line [22] (80% by volume in tissue), lipid[(a)], brown line [23] (20% by volume in tissue), lipid[(b)], pink line [24], melanin, black dashed line (http://omlc.ogi.edu/spectra/melanin/mua.html; μ_a corresponds to that in skin). Collagen (green line) and elastin (yellow line) spectra from [24].

- High contrast between blood and water/lipid.
- light-absorbing structures embedded in soft tissue.
- Gap between oxygenated and deoxygenated blood $\rightsquigarrow$ functional imaging
- Different wavelengths allow quantitative spectroscopic examinations
- Use of contrast agents for molecular imaging.

from: Paul Beard, 2011. "Biomedical photoacoustic imaging", *Interface Focus*.

PAT Applications: Breast Cancer Angiography

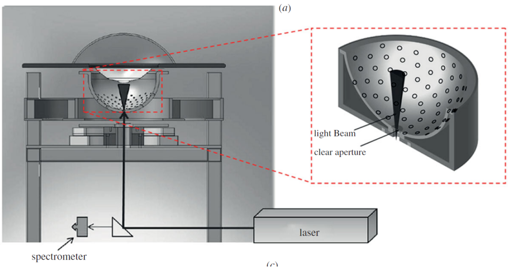

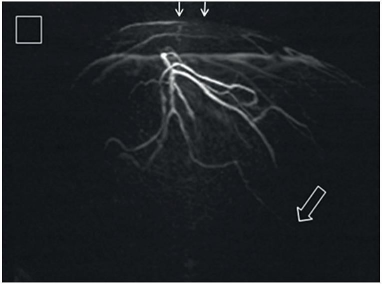

Kruger et al, 2010. "Photoacoustic angiography of the breast." *Med. Phys.*

PAT Applications: Skin Cancer Angiography

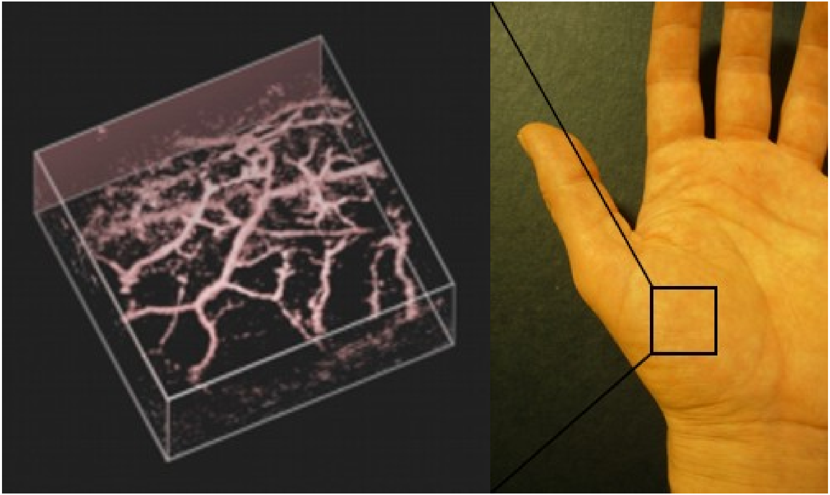

taken from: http://www.medphys.ucl.ac.uk/research/mle/images.htm

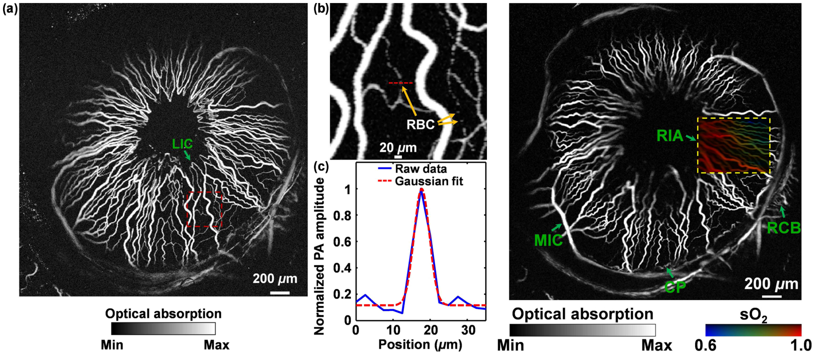

Hu et al., 2010. "Label-free photoacoustic ophthalmic angiography", *Optics Letters*

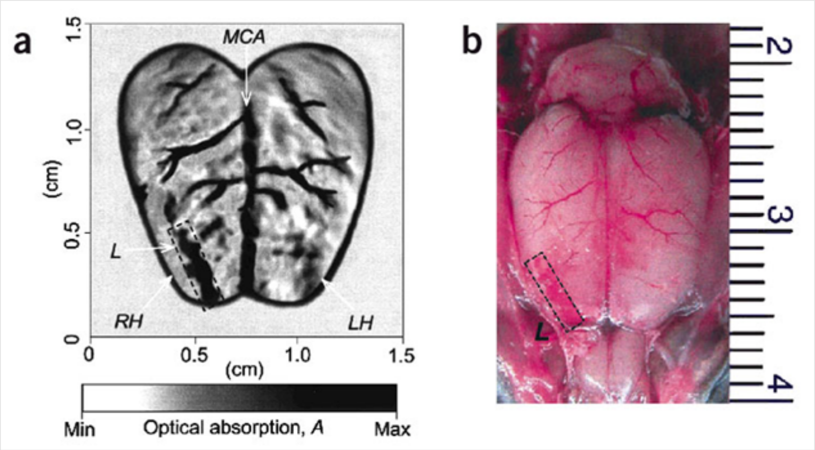

source: Wikimedia Commons

Wang et al., 2003. "Non-invasive laser-induced photoacoustic tomography for structural and functional imaging of the brain in vivo". *Nature Biotechnology*.

PAT Applications: Functional Brain Imaging

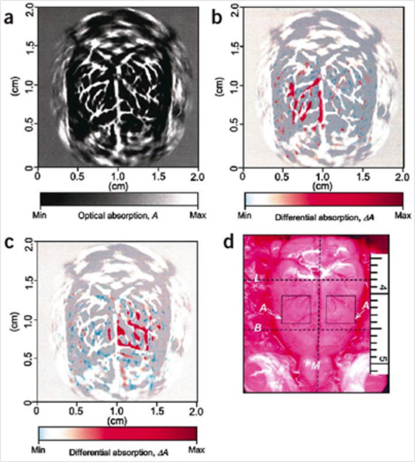

source: Wikimedia Commons

"Functional imaging of cerebral hemodynamic changes is response to whisker stimulation. (a) Noninvasive PAT image of the vascular pattern in the superficial layer of the rat cortex acquired with the skin and skull intact. The matrix size of the image was 1,000 (horizontal) X 1,000 (vertical), showing a 2.0 cm x 2,0 cm region. (b,c) Noninvasive functional PAT images corresponding to left-side and right-side whiskers stimulation, respectively, acquired with the skin and skull intact. These two maps of functional representations of whiskers are superimposed on the image of the vascular pattern in the superficial cortex shown in (a). (D) Open-skull photograph of the rat cortical surface. B, bregma; L, lambda; M, midline; A, activated regions corresponding to whisker stimulation (4 mm x 4 mm)."

Wang et al., 2003. "Non-invasive laser-induced photoacoustic tomography for structural and functional imaging of the brain in vivo". *Nature Biotechnology*.

PAT Applications: Human Brain Imaging

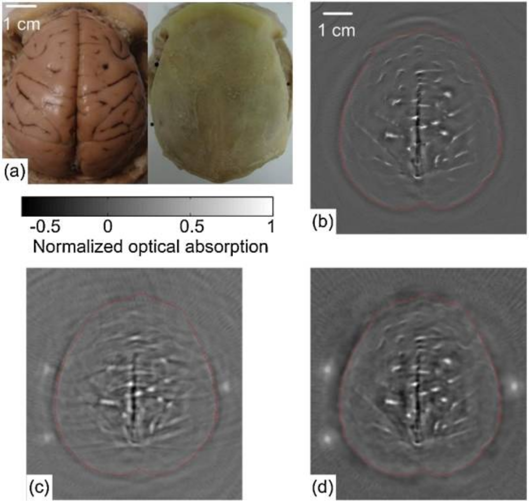

Huang et al., 2012. "Aberration correction for transcranial photoacoustic tomography of primates employing adjunct image data", *J. Biomed. Opt.*

PAT Applications: Intravascular Imaging

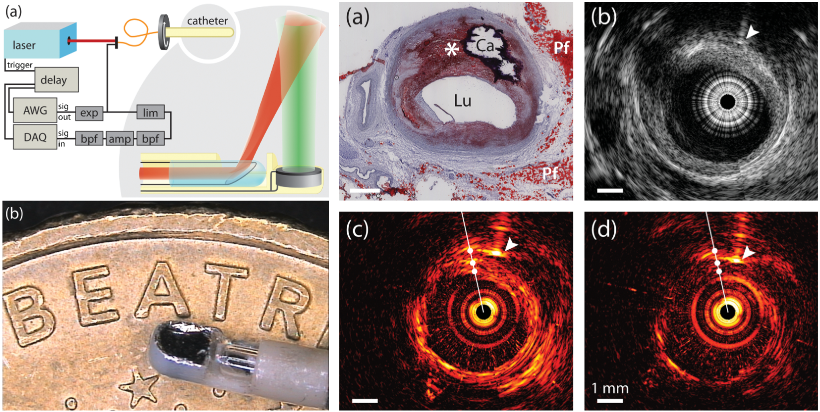

Jansen et al., 2011. "Intravascular photoacoustic imaging of human coronary atherosclerosis", *Optics Letters*

PAT as an "Imaging from Coupled Physics"-Technique

Traditional imaging modalities are often of either

- high contrast (healthy vs. unhealthy) but limited spatial resolution. (e.g. *optical tomography* (*OT*), *EIT*, *EEG/MEG*)

OR

- high spatial resolution but limited contrast. (e.g. *ultrasound*, *CT*, *MRI*)

Idea (hybrid imaging):

- Couple high contrast with high resolution modality
- Contrast induced by one modality is read out by the other.

Examples: (Q-)PAT, (Q-)*thermoacoustic tomography*, *ultrasound modulated*-EIT, *ultrasound modulated*-OT, *magnetic impedance*-EIT, *current density impedance imaging*

Caution: Multimodal imaging is NOT hybrid imaging!
(e.g., *PET-CT*, *PET-MRI*, *EEG-fMRI*,...)

- High resolution modalities typically lead to inverse problems that allow for an exact, analytical solution in the best case and can be solved in a stable way, otherwise.
- In low resolution modalities, coefficients or source terms of elliptic PDEs have to be recovered from boundary functionals of the solution $\Longrightarrow$ severely ill-posed inverse problems.
- In hybrid imaging, one first solves the "nice" high resolution problem and then solves an elliptic PDE from internal functionals of the solution $\Longrightarrow$ two moderately ill-posed inverse problems.

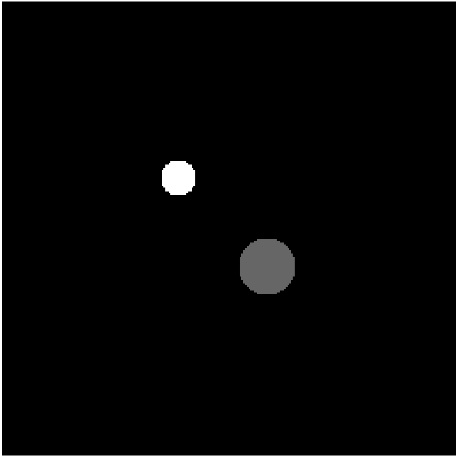

Energy absorption:

$$H = \mu_a \Phi$$

Initial pressure:

$$p_0 = \Gamma H$$

Wave propagation:

$$\Delta p - \frac{1}{c^2} \frac{\partial^2 p}{\partial^2 t} = 0$$

$$p|_{t=0} = p_0, \quad \frac{\partial p}{\partial t}|_{t=0} = 0$$

Caution: Initial value problems $\neq$ Scattering!

Taking Measurements

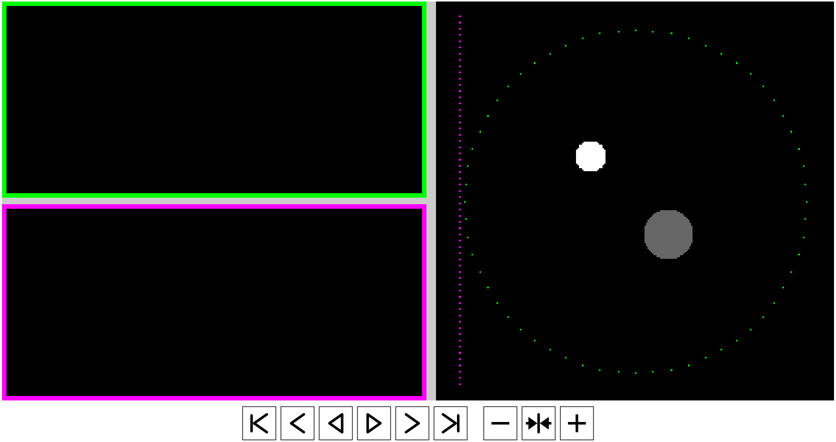

absorption coefficient: μ_a

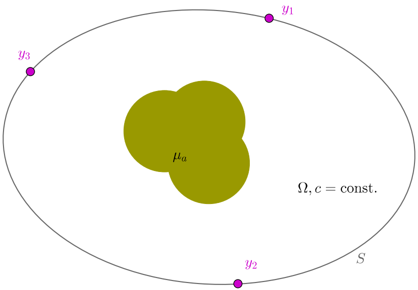

The Spherical Radon Transform

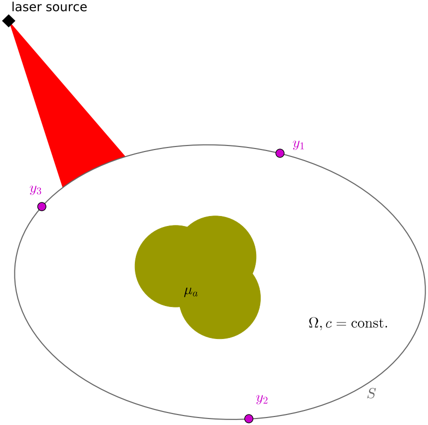

absorption coefficient: μ_a

pulsed laser excitation: Φ

The Spherical Radon Transform

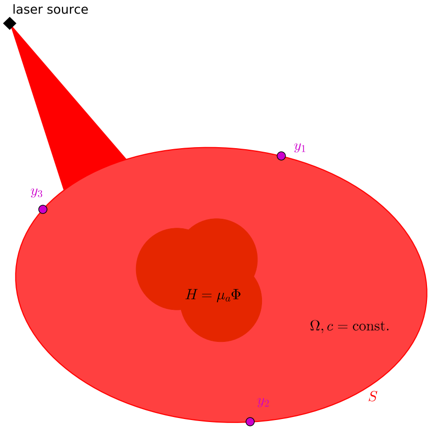

absorption coefficient: μ_a

pulsed laser excitation: Φ

thermal expansion:

$$H = \mu_a \Phi$$

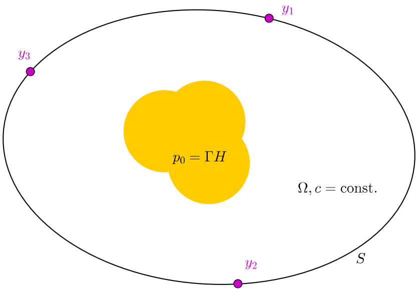

absorption coefficient: μ_a

pulsed laser excitation: Φ

thermal expansion:

$$H = \mu_a \Phi$$

initial pressure:

$$p_0 = \Gamma H$$

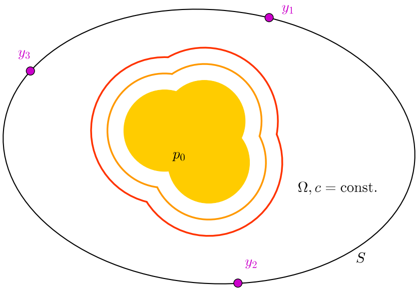

absorption coefficient: μ_a

pulsed laser excitation: Φ

thermal expansion:

$$H = \mu_a \Phi$$

initial pressure:

$$p_0 = \Gamma H$$

wave propagation:

$$\Delta p - \frac{1}{c^2} \frac{\partial^2 p}{\partial^2 t} = 0$$

$$p|_{t=0} = p_0, \quad \frac{\partial p}{\partial t}|_{t=0} = 0$$

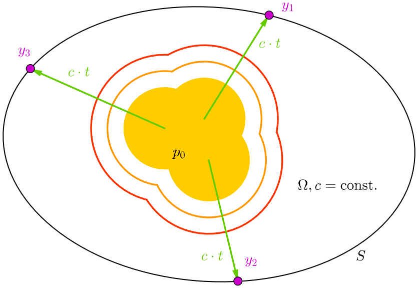

absorption coefficient: μ_a

pulsed laser excitation: Φ

thermal expansion:

$$H = \mu_a \Phi$$

initial pressure:

$$p_0 = \Gamma H$$

wave propagation:

$$\Delta p - \frac{1}{c^2} \frac{\partial^2 p}{\partial^2 t} = 0$$

$$p|_{t=0} = p_0, \quad \frac{\partial p}{\partial t}|_{t=0} = 0$$

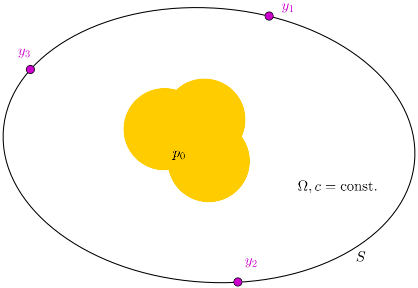

Let's change the perspective and focus on the sensors!

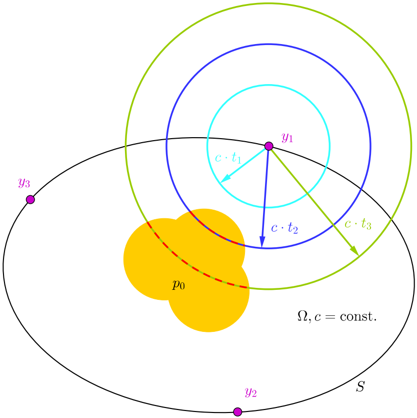

Assuming a homogenous sound speed, the PoissonâĂŞKirchhoff say that the measured signal g at a sensor at time t can be derived from the sum of all waves starting from a circle with radius $r = c \cdot t$:

$$\begin{aligned} g(y,t) &= C \frac{\partial}{\partial_t} t \int_{B_{ct}} p_0(x)\mathrm{d}x \\ &:= C \frac{\partial}{\partial_t} t \mathcal{A} p_0 \end{aligned}$$

$\mathcal{A}$ is called the spherical Radon transform.

$\Longrightarrow$ PAT inversion is basically a problem of integral geometry.

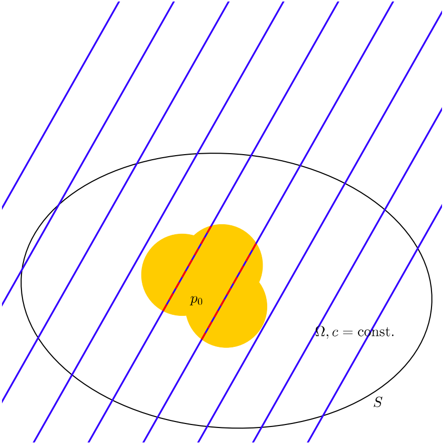

Thereby, PAT is similar to the classical Radon transform behind computed tomography (CT) where the measurements consist of line integrals of the quantity of interest:

$$g(\theta, s) = C \int_{\ell(\theta,s)} p_0(x)\mathrm{d}x$$

$$\ell(\theta, s) = \big\{(x_1, x_2) = (t\sin\theta + s\cos\theta, \\ -t\cos\theta + s\sin\theta) \,\big|\, t \in \mathbb{R}\big\}$$

Explicit Inversion Formulas

Eigenfunction expansion and closed-form filtered-backprojection-type approaches are available but often have restrictive assumptions on

- acoustic properties (homogenous sound speed)
- sensor geometries
- support of photoacoustic source
- optical absorption and dispersion
- computational resources

Relaxation of restrictions and incorporation of *a-priori* knowledge only in ad-hoc fashion.

P. Kuchment and L. Kunyansky, 2011., "Mathematics of Photoacoustic and Thermoacoustic Tomography", *Handbook of Mathematical Methods in Imaging*, Springer New York.

Time Reversal

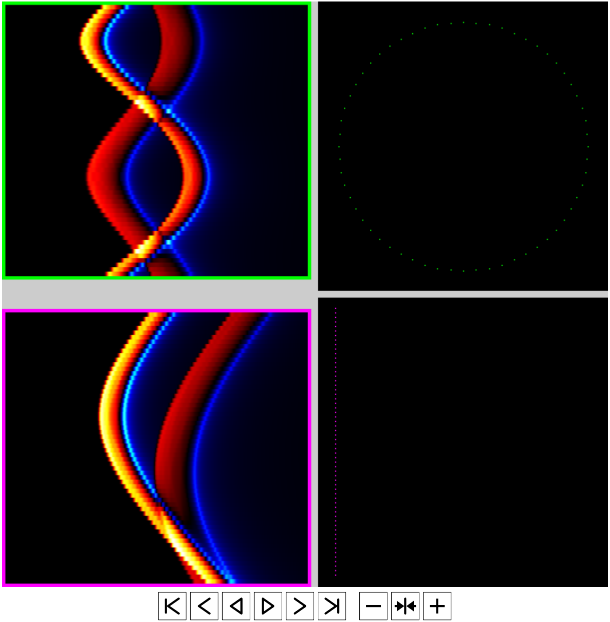

- Sending the recorded waves "back" into volume.
- "The least restrictive reconstruction algorithm for PAT".
- Needs a numerical model for acoustic wave propagation.

Acoustic Wave Propagation: Numerical Solution

We do not solve the wave equation but a system of first order conservation laws in the main acoustic variables including additional terms such as for modeling absorption and dispersion.

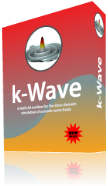

kWave$^{(*)}$ implements a k-**space pseudospectral method**:

- Compute spatial derivatives in Fourier space: 3D FFTs.
- Modify finite temporal differences by k-space operator.
- Use *staggered grids* for velocities.
- Incorporate *perfectly matched layer* to simulate free-space propagation.
- Parallel/GPU computing can lead to massive speed-ups.

$^{(*)}$B. Treeby and B. Cox, 2010. "k-Wave: MATLAB toolbox for the simulation and reconstruction of photoacoustic wave fields", *Journal of Biomedical Optics*

We gratefully acknowledge the support of NVIDIA Corporation with the donation of the Tesla K40 GPU used for this research.

All the steps of the numerical iteration to solve of the direct problem can be combined to a linear equation

$$f = Ap_0$$

One can derive a numerical adjoint iteration to have a representation of A^T (but its soooooo tedious*).

This allows to use variational regularization for image reconstruction:

$$\hat{p}_\lambda = \underset{p}{\operatorname{argmin}} \left\{ \frac{1}{2} \| Ap - f \|_2^2 + \lambda \mathcal{J}(p) \right\}$$

Solve by *conjugate gradient*, *proximal gradient algorithm* or *ADMM*.

(*) C. Huang, K. Wang, L. Nie, L.V. Wang, M.A. Anastasio, 2013. "Full-Wave Iterative Image Reconstruction in Photoacoustic Tomography With Acoustically Inhomogeneous Media", *IEEE Transactions on Medical Imaging*

A Simple Phantom

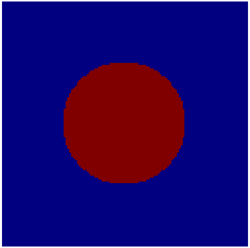

(a) Phantom

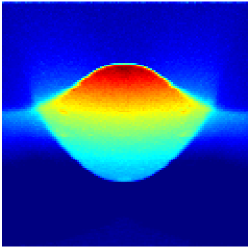

(b) Time reversal

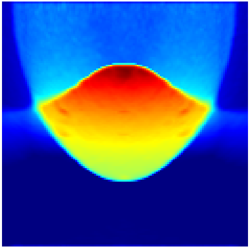

(c) $A^T f$

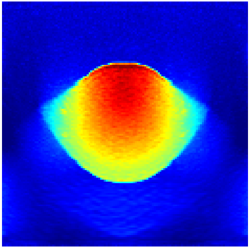

(d) Pseudo inverse (PI)

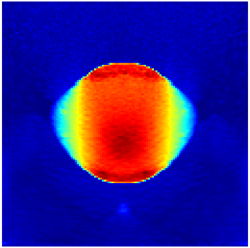

(e) PI + positivity

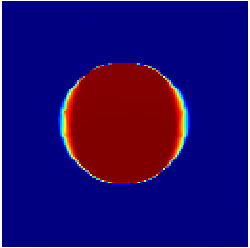

(f) TV + pos

Planar sensor on top, $n = 128^3$, SNR: 10. Maximum intensity projections, side view.

A More Realistic Phantom

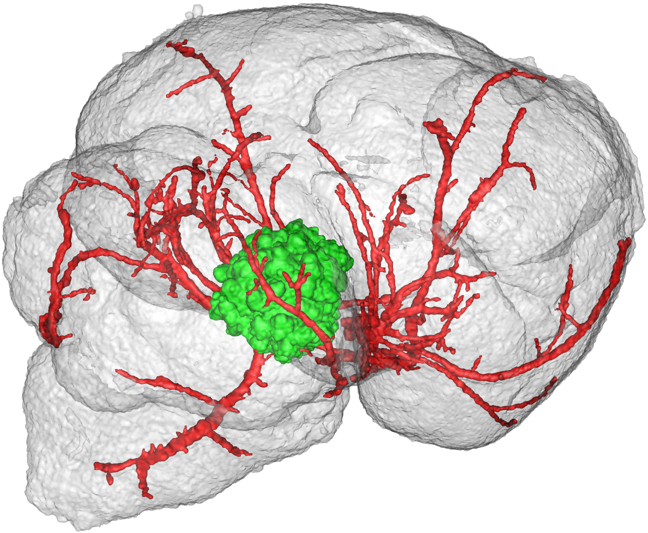

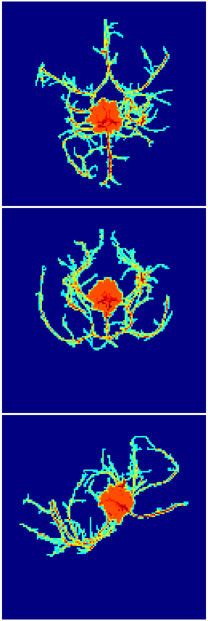

Time Reversal and Back Projection

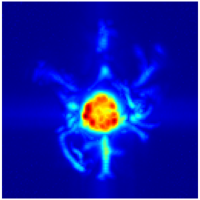

(g) TR, X

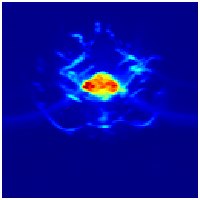

(h) TR, Y

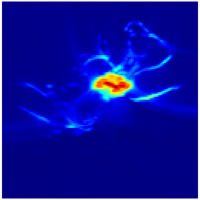

(i) TR, Z

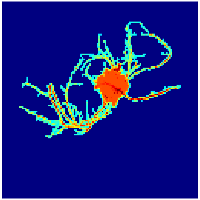

(j) Phantom, Z

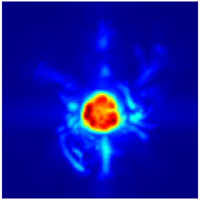

(k) BP, X

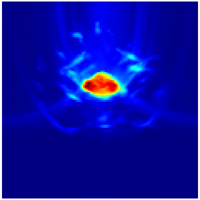

(l) BP, Y

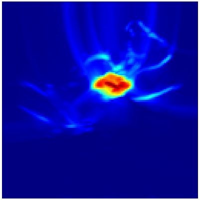

(m) BP, Z

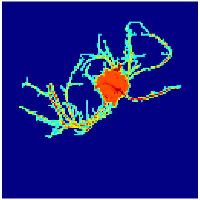

(n) Phantom, Z

Pseudo Inverse via CGLS (stopped by discrepancy principle)

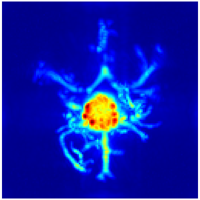

(a) PI, X

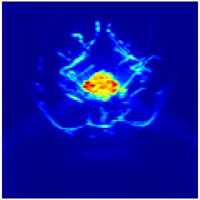

(b) PI, Y

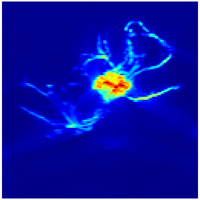

(c) PI, Z

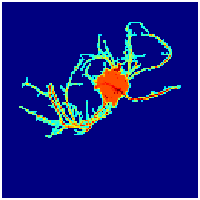

(d) Phantom, Z

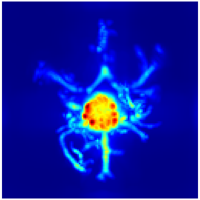

(e) PIppTV, X

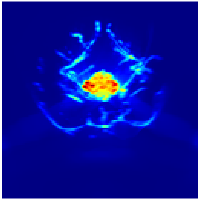

(f) PIppTV, Y

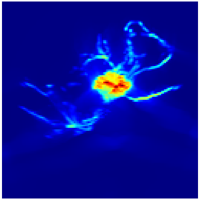

(g) PIppTV, Z

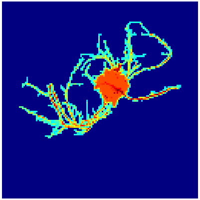

(h) Phantom, Z

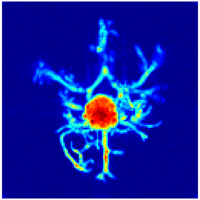
(a) PIPos, X

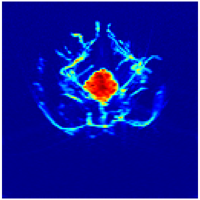
(b) PIPos, Y

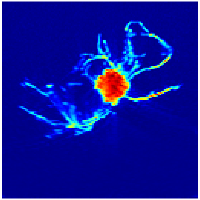
(c) PIPos, Z

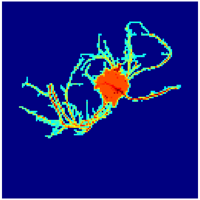
(d) Phantom, Z

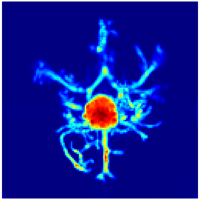
(e) PIPosppTV, X

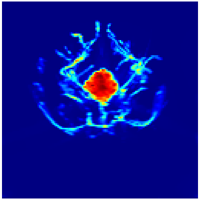
(f) PIPosppTV, Y

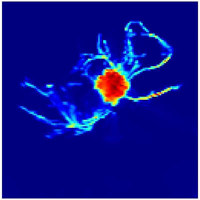
(g) PIPosppTV, Z

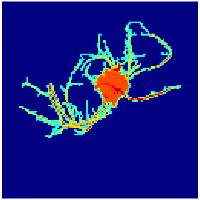
(h) Phantom, Z

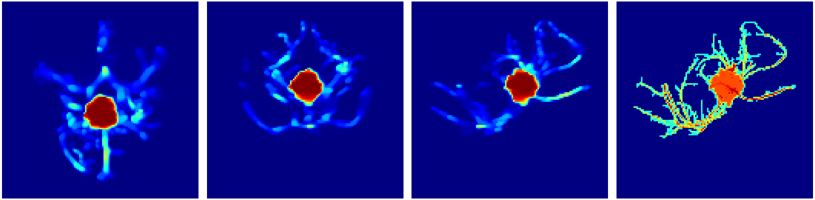

(a) TVregPos, X (b) TVregPos, Y (c) TVregPos, Z (d) Phantom, Z

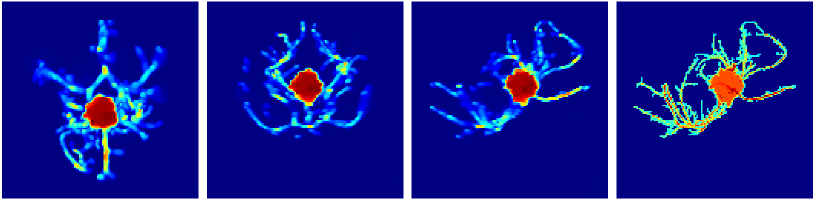

(e) TVbregPos, X (f) TVbregPos, Y (g) TVbregPos, Z (h) Phantom, Z

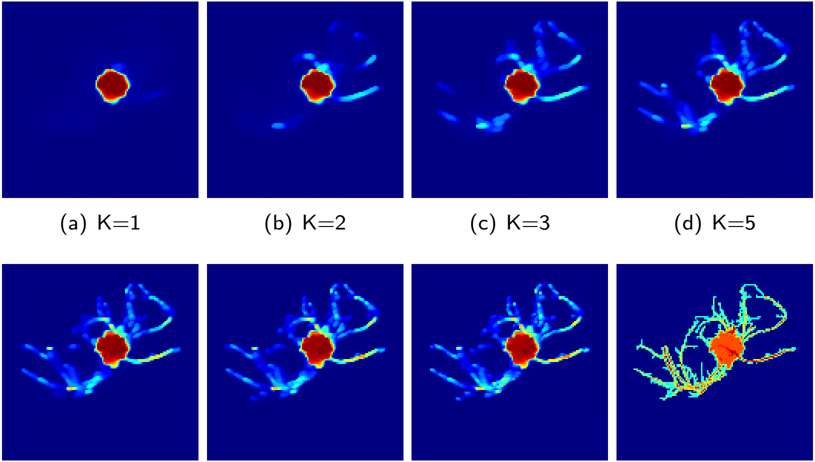

(a) K=1 (b) K=2 (c) K=3 (d) K=5

(e) K=8 (f) K=12 (g) K=20 (h) Phantom, Z

Experimental Phantom Data

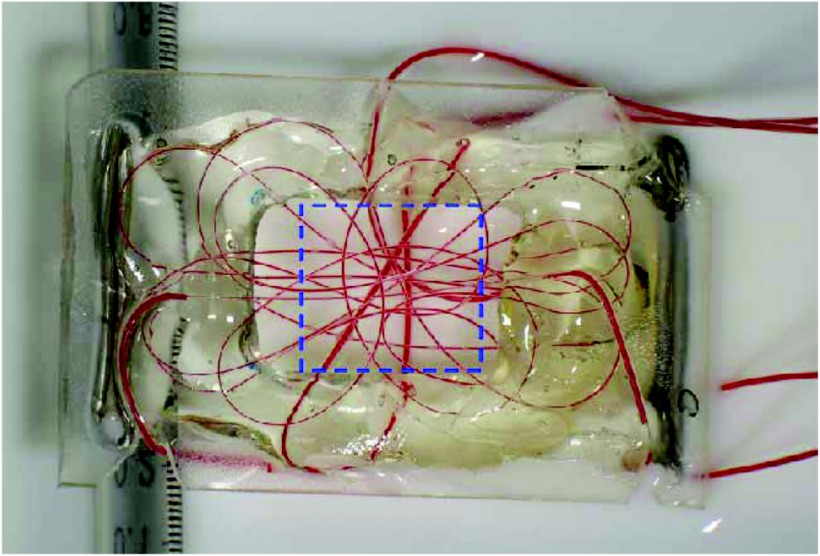

Time reversal: Raw and post-processed with TV denoising

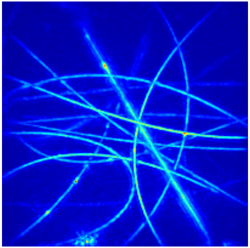

(a) TR, X

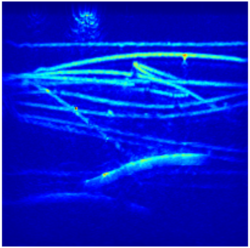

(b) TR, Y

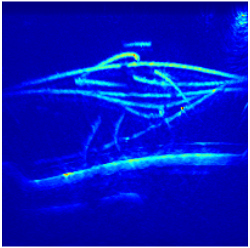

(c) TR. Z

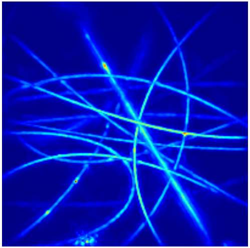

(d) TRppTV, X

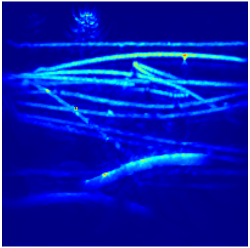

(e) TRppTV, Y

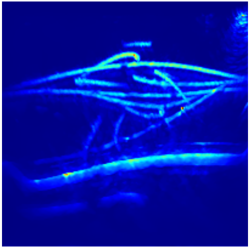

(f) TRppTV, Z

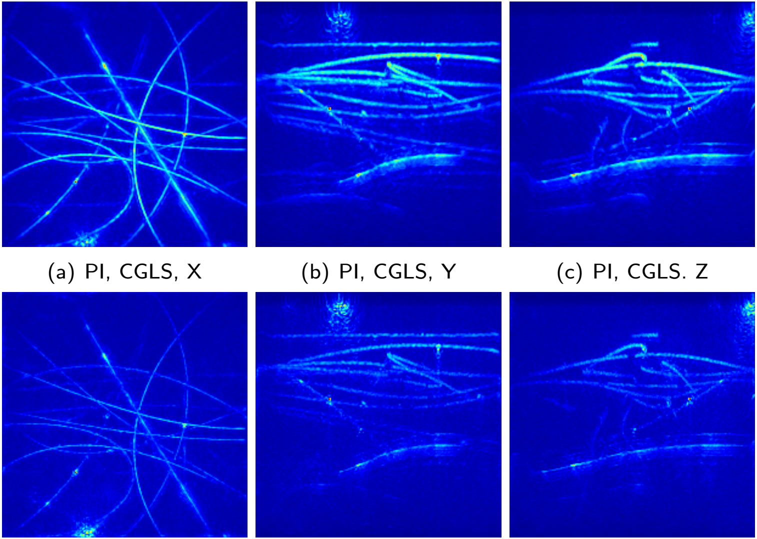

(a) PI, CGLS, X (b) PI, CGLS, Y (c) PI, CGLS. Z

(d) PI, grad, X (e) PI, grad, Y (f) PI, grad, Z

Positive Pseudo Inverse via Proximal Gradient (10 iterations)

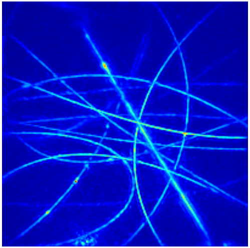

(a) PIPos, X

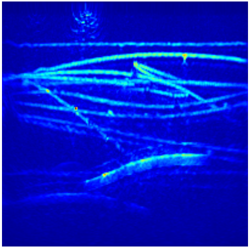

(b) Y

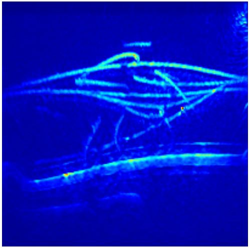

(c) Z

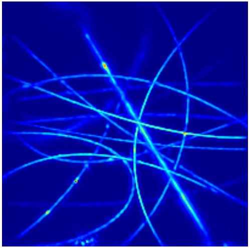

(d) PIPos, ppTV, X

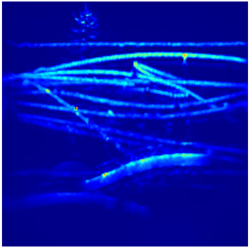

(e) Y

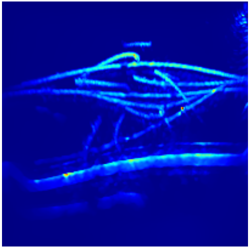

(f) Z

TV regularization + positivity (20 Iterations) vs TRpp

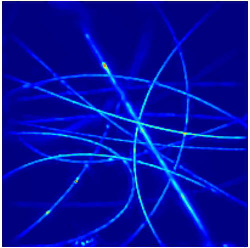

(a) TVPos, ProxGrad, X

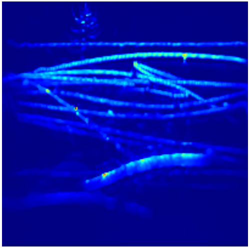

(b) Y

(c) Z

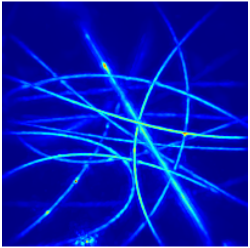

(d) TRppTV, X

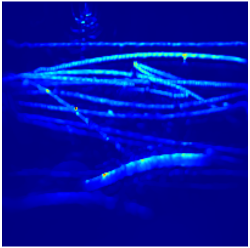

(e) Y

(f) Z

TV minimization + positivity via Bregman iterations

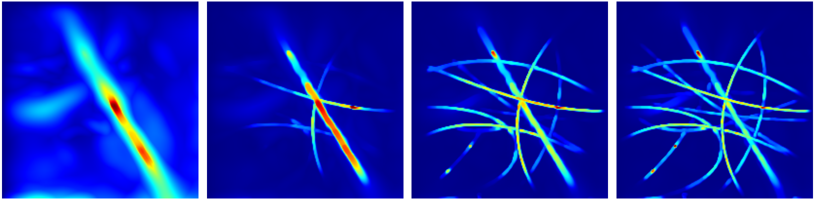

(a) K=1 (b) K=2 (c) K=3 (d) K=4

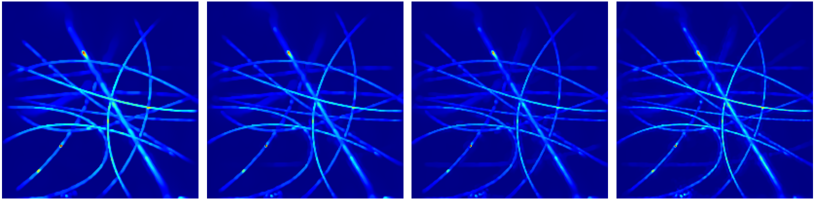

(e) K=6 (f) K=8 (g) K=10 (h) TVPos

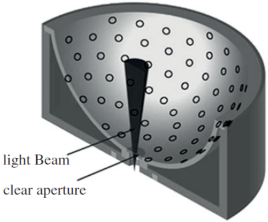

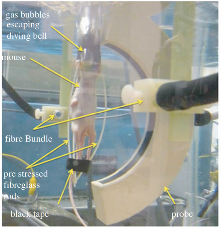

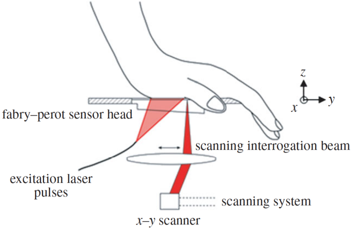

from: Paul Beard, 2011. "Biomedical photoacoustic imaging", *Interface Focus*.

Sensors for acoustic pressure:

- Piezoelectric arrays offer a high temporal, but only moderate spatial resolution. Flexible wrt geometry.
- Fabry Perot (FB) interferometer offer high spatial resolution and sensitivity but low temporal resolution. Restricted to planar geometries.

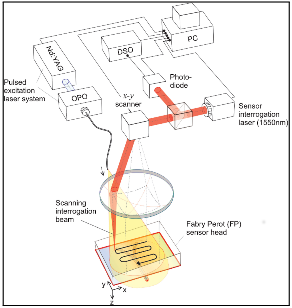

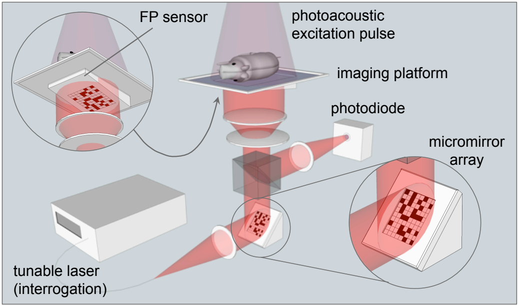

- Single-pixel sub-sampling (structured or random)
- Patterned interrogation by micromirror array, similar to ”single-pixel” Rice camera.

Mathematical formulation

$$f(t_i) = G(t_i)(Ap(t_i) + \varepsilon(t_i))$$

Frame-by-frame (*FBF*) reconstruction using sparsity constraints

$$\hat{p}_\lambda(t_i) = \operatorname*{argmin}_p \left\{ \frac{1}{2} \| G(t_i) A p - f(t_i) \|_2^2 + \lambda \mathcal{J}(p) \right\}$$

can already increase temporal resolution as less data is required.

Temporal redundancy of the data can be exploited by spatio-temporal regularization: Let $P = [p(t_1), \ldots, p(t_N)]$ and

$$\hat{P}_{\lambda,\mu} = \operatorname*{argmin}_P \left\{ \sum_i^N \frac{1}{2} \| G(t_i) A p(t_i) - f(t_i) \|_2^2 + \lambda \mathcal{J}(p(t_i)) + \mu \mathcal{H}(P) \right\}$$

- low-rank constraints: $\mathcal{H}(P) = \|P\|_*$ (nuclear norm).
- Decomposition models: $P = U + V$, $\mathcal{H}(P) = \mathcal{H}_1(U) + \mathcal{H}_2(V)$
- Visual flow or optimal transport constraints.

Summary

- PAT is an emerging biomedical "Imaging from Coupled Physics"-technique.
- Non-ionizing, high contrast for light-absorbing structures in soft tissue.
- Promising (pre-)clinical applications.
- Solve two moderate inverse problems instead of one severely ill-posed.
- Explicit solutions applicable to specific settings, only.
- Variational regularization approaches need computationally expensive explicit numerical representation of 3D wave propagation.
- High spatial resolution comes with slow data acquisition.

In our project, we try to overcome this limitation by combining recent advances in spatio-temporal sub-sampling schemes, compressed sensing and inverse problems with the development of tailored data acquisition systems.

A lot of work!

Thank you for your attention!

First order conservation laws:

$$\frac{\partial \mathbf{u}}{\partial t} = -\frac{1}{\rho_0}\nabla p \quad \text{(momentum conservation)}$$

$$\frac{\partial \rho}{\partial t} = -\rho_0 \nabla \cdot \mathbf{u} \quad \text{(mass conservation)}$$

$$p = c_0^2 \rho \quad \text{(pressure-density relation)}$$

with

u: acoustic particle velocity

ρ: acoustic density

ρ_0: ambient density

p acoustic pressure

c_0 isotr. sound speed

Can be combined to second order wave equation:

$$\Delta p - \frac{1}{c^2}\frac{\partial^2 p}{\partial^2 t} = 0$$

$$p|_{t=0} = p_0, \quad \frac{\partial p}{\partial t}|_{t=0} = 0$$

But: System of first order equations is advantageous for modeling and numerical accuracy.

Including heterogeneity and power law absorption and dispersion:

$$\frac{\partial \mathbf{u}}{\partial t} = -\frac{1}{\rho_0}\nabla p \quad \text{(momentum conservation)}$$

$$\frac{\partial \rho}{\partial t} = -\rho_0 \nabla \cdot \mathbf{u} - \mathbf{u} \cdot \nabla \rho_0 \quad \text{(mass conservation)}$$

$$p = c_0^2 \left(\rho + \mathbf{d} \cdot \nabla \rho_0 + L\rho\right) \quad \text{(pressure-density relation)}$$

$$L = \tau \frac{\partial}{\partial t} \left(-\Delta\right)^{\frac{y}{2}-1} + \nu \left(-\Delta\right)^{\frac{y+1}{2}-1} \quad \text{(integro-differential operator)}$$

$$\tau = -2\alpha_0 c_0^{y-1}, \quad \nu = 2\alpha_0 c_0^{y} \tan(\pi y/2) \quad \text{(absorption/dispersion coef.)}$$